This is the peer-reviewed, final accepted version for American Mineralogist, published by the Mineralogical Society of America.
The published version is subject to change. Cite as Authors (Year) Title. American Mineralogist, in press.
DOI: https://doi.org/10.2138/am-2021-7911. http://www.minsocam.org/

Revision 2

Copper isotope evidence for a Cu-rich mantle source of the world-class Jinchuan magmatic Ni–Cu deposit

YUN ZHAO[a, b], SHENG-AO LIU[a]*, CHUNJI XUE[a], MENG-LUN LI[a]

[a] *State Key Laboratory of Geological Processes and Mineral Resources, China University of Geosciences, Beijing 100083, China*

[b] *State Key Laboratory for Mineral Deposits Research, Nanjing University, Nanjing 210023, China*

Abstract words: ~340

Text words: ~5000

Figure#: 8

Table#: 1

References: 61

Supplementary material: 1

*Corresponding author. E-mail address: lsa@cugb.edu.cn

ABSTRACT

A Cu-rich mantle source may play a key role in generating giant magmatic Ni–Cu deposits worldwide, but evidence for source's Cu enrichment and its mechanism is still rare. Copper isotopes can provide novel and direct insights into this issue since metasomatism that causes Cu enrichment in the mantle is commonly associated with a huge Cu isotope fractionation. Here we present the first Cu isotopic study on the world-class Jinchuan magmatic Ni–Cu deposit in China, including disseminated, net-textured and massive sulfides. The disseminated and net-textured sulfides have variable δ^{65}Cu values (+0.36 ± 0.38‰, n=42), which are higher than those of massive sulfides (−0.44 ± 0.28‰, n=11). The country rocks have a narrow

This is the peer-reviewed, final accepted version for American Mineralogist, published by the Mineralogical Society of America.
The published version is subject to change. Cite as Authors (Year) Title. American Mineralogist, in press.
DOI: https://doi.org/10.2138/am-2021-7911. http://www.minsocam.org/

δ^{65}Cu range of 0.21‰ to 0.23‰, which is unlikely to have caused the large δ^{65}Cu variations. The absence of a relationship between δ^{65}Cu and whole-rock Cu contents rules out the possibility of surface weathering and diffusion-driven processes. Further, the lack of correlation between δ^{65}Cu and whole-rock Cu/Ni and Pd/Ir ratios excludes the large Cu isotopic variations as a result of progressive evolution of parental magma or sulfide melt. Numerical modeling indicates that the initially segregated sulfide melt has a mean δ^{65}Cu of 0.44 ± 0.22‰ (2SD). Sulfide-liquid fractionation could have contributed to the enrichment of ^{65}Cu in the Cu-rich net-textured sulfides and depletion of ^{65}Cu in massive sulfides, respectively. The fractionated sulfide melts were fragmented and assimilated by new magma pluses, and consequently, the new segregated sulfide melts acquired lighter and more variable δ^{65}Cu values in comparison with the initially accumulated sulfide melts. The estimated Cu isotopic composition of parental magmas for the Jinchuan Ni–Cu deposit is 0.54 ± 0.22‰ (2SD), which is up to ~0.5‰ higher than the mantle value. Copper transportation from oxidized subducted slabs to mantle peridotites and/or dissolution of Cu-bearing sulfides in the mantle caused oxidative breakdown and reprecipitation of sulfides, and shifted the hybridized mantle source toward heavy δ^{65}Cu as previously observed in mantle xenoliths. Our study therefore suggests that source's pre-enrichment is a key step in the generation of giant magmatic Ni–Cu deposits.

Keywords: Copper isotopes; Initial Cu enrichment; Mantle metasomatism; Magmatic Ni–Cu deposits

INTRODUCTION

Magmatic Ni–Cu deposits have produced some of the world's most valuable economic metals (Naldrett 2010; Barnes and Lightfoot 2005), including ~56% of the world's Ni production, ~3% of Cu production, and > 96% of platinum-group element (PGE) production. The generation of magmatic Ni–Cu deposits can be envisaged as four stages: (1) mantle melting to generate primary magmas, (2) minor sulfide removal or olivine crystallization during magma ascent, (3) significant sulfide segregation and coalescence in a dynamic magmatic conduit, and (4) internal fractionation of sulfide melt (Naldrett 2010). Mantle melting to generate primary magmas is the first and a key step, even though an efficient collection of metals by sulfides promotes full maturity of magmatic Ni–Cu deposits at shallow crustal levels (Barnes and Lightfoot 2005;

This is the peer-reviewed, final accepted version for American Mineralogist, published by the Mineralogical Society of America.
The published version is subject to change. Cite as Authors (Year) Title. American Mineralogist, in press.
DOI: https://doi.org/10.2138/am-2021-7911. http://www.minsocam.org/

Naldrett 2010). Especially, metasomatism is thought to introduce metals into the mantle via slab-derived fluid and/or melts (Fiorentini and Beresford 2008), and generate a metal-rich mantle source (e.g., Richardson and Shirey 2008; Griffin et al. 2013; Mungall and Brenan 2014). To date, geochemical evidence for a metal-rich mantle source largely relies on trace elements (e.g., Pt/Pd) and radiogenic Sr–Nd–Re–Os isotopes instead of isotopic systematics of the ore-forming metals (e.g., Maier and Barnes 2004; Zhang et al. 2008; Richardson and Shirey 2008). Therefore, possible metal enrichment in the mantle sources of magmatic Ni–Cu deposits is still poorly constrained, in particular from ore-forming metal isotopes.

In recent years, Cu isotope behaviors during mantle metasomatism, partial melting of mantle sources, and magma differentiation have been well established (e.g., Liu et al. 2015, 2019; Savage et al. 2015; Huang et al. 2016a, 2017; Wang et al. 2019). Oxidative breakdown and reprecipitation of sulfides during mantle metasomatism can cause significant Cu isotope fractionation, as widely observed in mantle peridotites and pyroxenites (e.g., Liu et al. 2015; Wang et al. 2019). For instance, some of metasomatized mantle peridotites have much higher $\delta^{65}Cu_{\text{NIST 976}}$ values (up to +1.82‰) than that of the primitive mantle (0.06 ± 0.20‰; Liu et al. 2015). High $\delta^{65}Cu$ values in some of orogenic and xenolith peridotites (up to +0.61‰) were also proposed to have resulted from melt–peridotite interaction (Huang et al. 2017). These observations suggest that Cu isotopes have potential as a tracer for Cu enrichment in the mantle sources of magmatic Ni–Cu deposits. To date, large $\delta^{65}Cu$ variations (~4‰) in worldwide magmatic Ni–Cu deposits have been observed, including Noril'sk Province, Russia (Malitch et al. 2014), Midcontinent Rift System, America (Ripley et al. 2015), Eastern Gabbro, Canada (Brzozowski et al. 2020), Tulaergen (Zhao et al. 2017, 2019), Kalatongke and Baishiquan (Tang et al. 2020), China. However, the mechanism that caused these large Cu isotopic variations has not yet been well constrained.

To investigate whether or not mantle metasomatism induced significant metal accumulation during generation of magmatic Ni–Cu deposits, here we carry out a systematical study of Cu isotopes along with PGE on the world-class Jinchuan Ni–Cu deposit, China. This deposit is the third largest magmatic Ni–Cu deposits in the world (Li and Ripley 2011), containing >500 million metric tons (Mt) of sulfide ores with average grades of 0.7 wt% Cu and 1.1 wt% Ni (Tang et al. 2009). The primary magmas of the Jinchuan intrusion were proposed to have been derived from an enriched subcontinental lithosphere mantle (SCLM)

This is the peer-reviewed, final accepted version for American Mineralogist, published by the Mineralogical Society of America.
The published version is subject to change. Cite as Authors (Year) Title. American Mineralogist, in press.
DOI: https://doi.org/10.2138/am-2021-7911. http://www.minsocam.org/

source (Li et al. 2005; Li and Ripley 2011; Zhang et al. 2013). In this contribution, our Cu isotope results suggest that the mantle source region of the Jinchuan deposit experienced initial Cu enrichment caused by metasomatism, and that this process probably plays a key role in generation of giant magmatic Ni–Cu deposits worldwide.

GEOLOGICAL SETTING AND SAMPLE DESCRIPTION

The Jinchuan mineralized intrusion is located in the NW-striking Longshoushan terrane in southern Alxa, the southwestern margin of the North China Craton (Fig. 1a, Song et al. 2009; Mao et al. 2018; Ding et al. 2021). In the Longshoushan terrane, Neoproterozoic and Paleozoic strata, including sandstones, limestones, and conglomerates unconformably overlie Paleo-Mesoproterozoic metamorphic units (e.g., Li and Ripley 2011; Chen et al. 2013). The Jinchuan intrusion is 6000 m long and 300 m wide, and the downward extension is >1000 m in the central part (Fig. 1b). It is composed of Segment III, Segment I, Segment II, and Segment IV from west to east (Fig 1b, c). The four segments are divided by a series of strike-slip faults, named F8, F16, F17 and F23 (Fig. 1b, c).

The Jinchuan intrusion was emplaced into the Proterozoic suite of migmatites, gneiss and marble (Fig. 1). Segment I intrudes into the marble, and Segment II is emplaced along the boundary between the migmatites and marble (e.g., Chen et al. 2013). Both Segment III and Segment IV intrude into migmatites. These segments occur as SE-trending dikes, parallel to the regional structures (Fig. 1). Dunite, lherzolite, and olivine websterite are the dominant rock types of the Jinchuan intrusion (Li and Ripley 2011; Chen et al. 2013). In the outcrops, lherzolite is widespread, and olivine websterite occurs along the margin of lherzolite (Fig. 1). Only minor dunite is located in the northwest part of the Segment I on the surface (Fig. 1a). By contrast, sulfide-mineralized dunite is much more common in drill cores. These different types of rocks in the Jinchuan intrusion have gradational boundaries (Mao et al. 2019).

Sulfide mineralizations in the Jinchuan deposit consist of disseminated (Fig. 2a), net-textured (Fig. 2b), and massive types (Fig. 2c), among which net-textured and disseminated types are most abundant. Vein-like massive sulfide orebodies crosscut disseminated and net-textured sulfide orebodies in some places. The disseminated sulfides are hosted by dunite and lherzolite, whereas net-textured sulfides are commonly

associated with dunite. Disseminated and net-textured sulfides occur as spotted or net-like shapes, respectively (Fig. 2a–b). Sulfide minerals in the Jinchuan deposit include pyrrhotite, pentlandite and chalcopyrite (Fig. 2d).

Disseminated, net-textured and massive sulfides as well as country rocks were collected from underground adits of 1040 m and 1220 m elevations in Segment I and Segment II (Table S1, Figs. 1, 4 and 5). Except for the country rocks, fresh samples with more than 6 wt.% sulfide were collected for separating chalcopyrite.

ANALYTICAL METHODS

Analysis of Cu, Ni, PGE, and S contents

The whole-rock Cu, Ni, PGE, and S contents of different types of sulfide ores and country rocks from the Jinchuan deposit were measured at the National Research Center of Geoanalysis, China. Samples for Cu and Ni content analysis were powdered and then digested in a mixture of HF and HNO_3 in Teflon bombs. The measurement was conducted by a MAT ELEMENT ICP–MS, following the procedures established by Balaram et al. (1995). The accuracy and reproducibility were better than ±10% and 2%−10% in terms of relative standard deviation (RSD), respectively. Sulfur contents were analyzed by a high-frequency infrared carbon sulfur analyzer (HIR 944). Reproducibility was better than 10% RSD, and the accuracy was better than ±5%. The PGE contents measurement utilized a NiS-bead pre-concentration and Te co-precipitation, following by ICP–MS analysis, using an established procedure modified from Asif and Parry (1991). The measurements were monitored using standards of UMT-1 and WPR-1. The analytical accuracy and reproducibility were better than ±10% and 10% RSD, respectively.

Analysis of Cu isotopes

The chalcopyrite grains in each sample were checked under a microscope to avoid visible inclusions. In order to check the purity of studied chalcopyrites prior to isotopic analysis, Cu/Fe ratios of chalcopyrites were firstly determined by an ICP–OES, with reproducibility better than ±5%. Sample digestion, chemical purification, and isotope measurement followed the established procedures of Liu et al. (2014a).

This is the peer-reviewed, final accepted version for American Mineralogist, published by the Mineralogical Society of America.
The published version is subject to change. Cite as Authors (Year) Title. American Mineralogist, in press.
DOI: https://doi.org/10.2138/am-2021-7911. http://www.minsocam.org/

Approximately 0.1 mg chalcopyrite grains and 25 mg reference materials (basalt, BHVO-2) were weighted and then digested in a mixed solution of HNO_3 and HCl acids. After complete dissolution of the samples, 1 mL of 8 N HCl + 0.001% H_2O_2 was added to the Teflon vessels and evaporated to dryness at 80 °C. This procedure was repeated three times prior to anion exchange chromatography. Copper was separated by pre-cleaned AG-MP-1M ion exchange resin. The collected solution was evaporated to dryness and re-dissolved, and column chemistry was performed twice for further purification. The Cu yields when processed twice through column chemistry were better than 99.7%, and the procedural blanks were <2 ng. Each purified sample was evaporated and then re-dissolved in 3% HNO_3 to remove the chloride ion prior to isotope measurement.

Copper isotope ratios were measured using a *Neptune plus* MC–ICP–MS at the China University of Geosciences, Beijing, China. Conventional sample–standard bracketing method was utilized for mass bias correction. Copper isotope data are reported in δ-notation relative to standard NIST 976 (Equation 1):

$$\delta^{65}Cu = (({}^{65}Cu / {}^{63}Cu)_{sample} / ({}^{65}Cu / {}^{63}Cu)_{NIST\ 976} - 1) \times 1000 \quad (1)$$

Long-term external reproducibility was ±0.05‰ for $\delta^{65}Cu$ (2SD) on the basis of repeated analysis of geostandards and synthetic solutions. In this analytical session, analysis of BHVO-2 yielded $\delta^{65}Cu = 0.11 \pm 0.05$‰ (2SD) and $\delta^{65}Cu = 0.09 \pm 0.05$‰ (2SD), which is in good agreement with the published ranges for this standard (Liu et al. 2014a, 2015; Sossi et al. 2015).

RESULTS

Whole-rock Cu, Ni, PGE and S contents, and Cu isotopic compositions of chalcopyrites and country rocks are reported in Supplementary Table S1 and Figures 3–5.

Cu, Ni, PGE, and S contents

Similar Cu/Ni and Pd/Ir ratios in disseminated and net-textured sulfide ores were observed in Segment I and Segment II (Fig. 4b–c). Massive sulfide ores have lower Pd/Ir ratios and more variable Cu/Ni ratios than disseminated and net-textured sulfides. In the primitive mantle-normalized diagrams, disseminated and net-textured sulfides have similar PGE patterns with depletion in Os, Ir, and Ru and enrichment in Rh, Pt,

and Pd, except for Pt anomalies in some samples (Fig. 4d–f). Massive sulfide ores have flat PGE patterns, except for Pt anomalies. These samples have higher PGE contents than the disseminated and net-textured sulfide ores (Fig. 4d–f). The possibilities for Pt anomaly include crystallization of sperrylite prior to solidification of the sulfide melts and preferential Pt enrichment into the Cu-rich residual sulfide melts (e.g., Chen et al. 2013).

Copper isotopes

The Cu/Fe ratios of chalcopyrite separates range from 0.90 to 1.13 (Table S1), which is consistent with stochiometric chalcopyrite (~1). This indicates that all samples analyzed in this study are magmatic chalcopyrite without secondary Cu-bearing minerals. The δ^{65}Cu values of disseminated and net-textured sulfides are between −0.47‰ and +1.29‰, with a mean of +0.36‰. There is no systematical change of δ^{65}Cu values in disseminated and net-textured sulfides from Segment I to Segment II (Fig. 5). The Cu isotopic composition of massive sulfides is much lighter than disseminated and net-textured sulfides, varying from −0.91‰ to +0.09‰ with a mean of −0.44‰. The country rocks of the Jinchuan deposit have a narrow range of δ^{65}Cu from +0.21‰ to +0.23‰, with a mean of +0.22‰ (n=4, migmatite and gneiss). Four chalcopyrite separates were repeated by dissolving a new aliquot, yielding Cu isotope compositions identical with the original measurements (Table S1; Fig. 5). The disseminated and net-textured sulfide ores of the Jinchuan deposit have elevated δ^{65}Cu values compared with sulfide ores in other magmatic Ni–Cu deposits (except for Midcontinent Rift System, Ripley et al. 2015), bulk silicate Earth (BSE) and non-metasomatized peridotites, but fall within the δ^{65}Cu range of metasomatized peridotites (−0.64‰ to +1.82‰, Fig. 3).

DISCUSSION

Possible origins of Cu isotopic variations in Jinchuan sulfides

Mantle melting to generate primary magmas is the first and a key step in the generation of magmatic Ni–Cu deposits (Barnes and Lightfoot 2005; Naldrett 2010). Global non-metasomatized mantle peridotites have a narrow range of δ^{65}Cu (0.03‰ ± 0.24‰, Liu et al. 2015) that are identical to those of basaltic rocks, regardless of varying degrees of partial melting (Liu et al. 2015; Savage et al. 2015; Huang et al. 2016a;

Moynier et al. 2017). The preferential release of ^{65}Cu during alteration and weathering produces ^{63}Cu enrichment in the residual rocks (Mathur et al. 2005; Liu et al., 2014b), which is in contrast to the elevated δ^{65}Cu values of Jinchuan sulfides. The lack of correlation between δ^{65}Cu and whole-rock Cu contents (Fig. 7b) further argues against any significant loss of isotopically light Cu by alteration and weathering. The remaining mechanisms that may induce significant fractionation of Cu isotopes are: (1) crustal contamination; (2) diffusion; and/or (3) sulfide segregation and internal fractionation within cumulated sulfide melts. We discuss these possibilities in turn below.

Crustal contamination. Crustal contamination during magma ascent, emplacement, and differentiation has occurred during the generation of the Jinchuan deposit (Ripley et al. 2005; Tang et al. 2018). Average continental crust contains ~30 ppm Cu (Rudnick and Gao 2003), two times lower than that of basaltic/picritic magmas (~90 ppm Cu, Lee et al. 2012), the latter of which was considered to be the primary magmas for the Jinchuan deposit (Barnes and Lightfoot 2005; Li and Ripley 2011; Chen et al. 2013). Thus, contamination by crustal materials during magma ascent, if any, has not significantly changed Cu isotopic compositions of the magmas. More importantly, the δ^{65}Cu of the continental crust (around zero, Li et al. 2009) is indistinguishable from non-metasomatized peridotites (0.03‰ ± 0.24‰, Liu et al. 2015). The assimilation of marbles may have induced sulfide saturation in the Jinchuan Ni–Cu sulfide deposit (Tang et al., 2018; Ding et al., 2021). However, marble is poor in Cu, and the assimilation of marbles causes negligible Cu isotopic variation. Also, migmatites and gneiss in the Jinchuan area are characterized by restricted Cu isotopic compositions of +0.21‰ to +0.23‰ (Fig. 5), which is unlikely to have caused the large δ^{65}Cu variation observed in the Jinchuan sulfides. Collectively, crustal contamination is not responsible for the ^{65}Cu enrichment in disseminated and net-textured sulfides in Jinchuan.

Diffusion. Copper isotopes may be fractionated by diffusion-driven processes with thermal or chemical gradients (e.g., Williams and Archer 2011). Here, at least two lines of evidence do not support diffusion-driven isotopic effects in Jinchuan sulfides. First, if diffusion effects happened, massive sulfides with high Cu contents should have heavier δ^{65}Cu values than those of disseminated and net-textured sulfides with low Cu contents, because lighter isotopes move faster than heavier ones (e.g., Richter et al. 2003). By contrast, massive sulfides in Jinchuan are enriched in lighter Cu isotope (Figs. 5, 7b). Second, there is no

This is the peer-reviewed, final accepted version for American Mineralogist, published by the Mineralogical Society of America.
The published version is subject to change. Cite as Authors (Year) Title. American Mineralogist, in press.
DOI: https://doi.org/10.2138/am-2021-7911. http://www.minsocam.org/

spatial Cu isotopic variation in disseminated sulfides from Segment I to Segment II (Fig. 5), precluding the possible diffusion-driven process that is expected to generate systematical variation in δ^{65}Cu values.

Sulfide segregation and fractionation within cumulated sulfide melts. Significant Cu isotope fractionation (up to 2.51‰) during sulfide segregation and internal sulfide fractionation has been reported in the Tulaergen deposit, China, and redox reactions were proposed to control the large δ^{65}Cu variations (Zhao et al. 2017, 2019). Sulfide melts segregated from primary or parental magmas preferentially incorporate lighter Cu isotopes relative to the coexisting silicate magmas as revealed by studies of igneous systems (e.g., Huang et al., 2016a), experiments (e.g., Savage et al. 2015; Xia et al. 2019), theoretical calculations (e.g., Liu et al., 2021), and magmatic Ni–Cu mineralization systems (e.g., Zhao et al. 2017, 2019). Sulfide fractionation would result in heavy Cu isotopes preferring Cu-rich sulfide melts to Fe-rich monosulfide solid-solution (MSS) (e.g., Zhao et al. 2019). Indeed, the massive ores have lighter Cu isotopic compositions than disseminated and net-textured sulfides in Jinchuan, which could be attributed to sulfide segregation and MSS–residual sulfide liquid fractionation (e.g., Zhao et al. 2017, 2019). The mass-balance equation (Equation 2, Campbell and Naldrett 1979) and the Rayleigh equation (Equation 3, Neumann et al. 1954) were used to simulate sulfide segregation (Stage II, Figs. 7, 8) and internal sulfide fractionation (Stage III, Figs. 7, 8), respectively.

$$C_S = C_M \times D \times (R + 1) / (R + D) \quad (2)$$

Where C_S = the metal concentration in sulfide melt; C_M = the metal concentration in silicate melt; D = sulfide-silicate melt partition coefficient; R factors = mass ratio of silicate magma to sulfide melts in equilibrium.

$$C_f = C_i \times F^{(D-1)} \quad (3)$$

Where C_f = metal concentration in fractionated sulfide melt; C_i = metal concentration in initial sulfide melt; D = bulk solid-liquid partition coefficient; F = the fraction of remaining sulfide melt.

Modeling results suggest that the parental magmas of the mineralized Jinchuan intrusion contain ~0.49 ppb Pd and ~0.14 ppb Ir, with R factors from ~500 to ~2700. Variable degrees of sulfide-melt fractionation formed Fe-rich massive and Cu-rich net-textured sulfide ores (Fig. 6). The parental magmas of the Jinchuan intrusion have higher Pd and Ir contents than those of the Tulaergen deposit (~0.25 ppb Pd and ~0.003 ppb Ir;

Zhao et al. 2019) in the Tianshan orogenic belt.

Numerical calculations indicate that variable R factors may be responsible for large Cu isotope fractionation in the Kalatongke, Baishiquan and Eastern Gabbro magmatic Ni–Cu deposits (e.g., Tang et al. 2020; Brzozowski et al. 2020). However, the formation of the Jinchuan deposit has experienced both sulfide segregation with variable R factors and subsequent sulfide-liquid fractionation (Fig. 6), which was also proposed by Chen et al. (2013) based on PGE data. Considering that significant Cu isotope fractionation occurs during sulfide-liquid fractionation (e.g., Zhao et al. 2017, 2019), the large δ^{65}Cu range of the Jinchuan deposit is not simply controlled by variable R factors. Copper contents and Cu/Ni and Pd/Ir ratios in sulfide-saturated magma can be used as indicators of different evolution stages of parental magmas or sulfide melts (e.g., Barnes and Lightfoot 2005; Zhao et al. 2017, 2019), with higher Cu contents and higher Cu/Ni and Pd/Ir ratios in evolved magmas or sulfide melts (e.g., Barnes and Lightfoot 2005; Naldrett 2010). However, Cu isotopic ratios are not correlated with whole-rock Cu contents, Cu/Ni and Pd/Ir ratios in the Jinchuan deposit (Figs. 4, 5 and 7), indicating that they do not simply result from the progressively evolved parental magma or sulfide melt. Disseminated sulfides can mirror the nature of the parental magma (Barnes and Maier, 1999), which can be further utilized to estimate the Cu isotopic composition of parental magmas. Calculations using mass-balance (Equation 2) and Rayleigh (Equation 3) equations indicate that initial segregated sulfides (represented by disseminated sulfides) have been generated at ~2700 R-factors (Fig. 6), having a mean δ^{65}Cu value of 0.44 ± 0.22‰ (Table 1, Figs. 3 and 7). By contrast, the initial sulfide melts of the Tulaergen deposit derived from the depleted mantle have δ^{65}Cu values of −0.54 ± 0.41‰ (Zhao et al. 2019).

Calculations using the Rayleigh distillation equation (Equation 4) suggest that variable degrees of sulfide-liquid fractionation (Stage III, Figs. 7, 8) contributed to the enrichment of ^{65}Cu in the Cu-rich net-textured sulfides (δ^{65}Cu value up to 1.29‰) and the enrichment of ^{63}Cu in the massive sulfides (δ^{65}Cu value as low as −0.91‰).

$$\delta_f = (\delta_i + 1000) \times (1 - f^{\alpha}) / (1 - f) - 1000 \quad (4)$$

Where δ_i = the δ^{65}Cu values in sulfide melt/magma; δ_f = the δ^{65}Cu values in sulfide melt or magma when a fraction (f) of Cu is left; f = the fraction of remaining Cu. Isotopic fractionation factor α is defined

This is the peer-reviewed, final accepted version for American Mineralogist, published by the Mineralogical Society of America.
The published version is subject to change. Cite as Authors (Year) Title. American Mineralogist, in press.
DOI: https://doi.org/10.2138/am-2021-7911. http://www.minsocam.org/

as:

$$\alpha^{65}Cu_{\text{residual sulfide melt–sulfide melt}} = (1000 + \delta_{\text{residual sulfide melt}}) / (1000 + \delta_{\text{sulfide melt}}) \quad (5)$$

$$\alpha^{65}Cu_{\text{MSS–sulfide melt}} = (1000 + \delta_{\text{MSS}}) / (1000 + \delta_{\text{sulfide melt}}) \quad (6)$$

$$\alpha^{65}Cu_{\text{sulfide melt–magma}} = (1000 + \delta_{\text{sulfide melt}}) / (1000 + \delta_{\text{magma}}) \quad (7)$$

The concentrated sulfide melts were fragmented and assimilated by new magma pluses continuously, accompanied by the second stage of scavenging of metals, sulfide segregation, internal sulfide fractionation, and sulfide percolation (Stage IV, Figs. 7, 8). This hypothesis is consistent with previous explanations that the formation of the Jinchuan intrusion has involved multiple magma influxes (e.g., Li and Ripley 2011; Chen et al. 2013; Mao et al. 2018). The new segregated sulfide melts have lighter and more variable Cu isotopic compositions than the pre-existing sulfide melts (Stage IV, Figs. 7, 8) due to sulfide-magma differentiation (e.g., Zhao et al. 2017, 2019).

Evidence for a Cu-rich metasomatized mantle source in Jinchuan

The estimated $\delta^{65}Cu$ values of initial sulfide melt from the Jinchuan magmatic system (0.44 ± 0.22‰) are much heavier than that of the terrestrial mantle (Fig. 3). Experimentally determined Cu isotope fractionation factors between sulfide melt and silicate magma are controlled by Ni contents in sulfide, with higher Ni (~25 wt.%, $\Delta^{65}Cu_{\text{sulfide melt-magma}} = \sim -0.1‰$; Xia et al. 2019) displaying smaller fractionation than sulfides with lower Ni (0.1 to 1.2 wt.%, $\Delta^{65}Cu_{\text{sulfide melt-magma}} = 0.77 \times 10^6/T^2 - 4.46 \times 10^{12}/T^4$, where T is Kelvin temperature; Xia et al. 2019). In the experimental work of Savage et al. (2015), sulfide phases also preferentially incorporate lighter Cu isotopes relative to whole-rock Cu ($\Delta^{65}Cu_{\text{sulfide melt-whole-rock Cu}} = \sim -0.1‰$). The Ni contents in sulfide for the Jinchuan deposit are calculated using Equation 8 (e.g., Barnes and Lightfoot 2005), ranging from 1.9 to 21.1 wt.% with a mean of 9.3 wt.%.

$$C_{(100\%\ \text{sulfide})} = C_{\text{rock}} \times 100 / (2.527 \times S + 0.3408 \times Cu + 0.4715 \times Ni) \quad (8)$$

Where $C_{(100\%\ \text{sulfide})}$ = metal contents in sulfides; C_{rock} = metal contents in rocks; S, Cu, and Ni = S, Cu, and Ni contents in rocks (wt.%).

Based on these experimental studies, the Cu isotope fractionation factor between sulfide and magma ($\Delta^{65}Cu_{\text{sulfide melt-magma}}$) is assumed to be −0.1‰. We further estimated the Cu isotopic composition of the

297 parental magma for the Jinchuan intrusion, which yielded an average δ^{65}Cu value of 0.54 ± 0.22‰ (2SD,
298 Table 1). The Cu isotopic composition of the SCLM-derived Jinchuan deposit is much higher than that of
299 the depleted mantle-derived Tulaergen deposit (δ^{65}Cu = 0.06 ± 0.20‰, Zhao et al. 2019). Given that mantle
300 melting induces negligible Cu isotope fractionation (Liu et al. 2015; Huang et al. 2016a; Moynier et al.
301 2017), the significant enrichment of heavy Cu isotopes in the parental magmas of the Jinchuan deposit
302 should have been inherited from its mantle source.

303 Copper occurs as monovalent and divalent in nature, with high-valence Cu-bearing minerals enriched
304 in heavy isotopes due to its redox-sensitive affinities (Mathur et al. 2005). In the range of oxygen fugacities
305 for igneous rocks, the Cu valence state remains +1 (e.g., Ripley et al. 2002). Accordingly,
306 non-metasomatized peridotites have restricted Cu isotopic composition close to zero (Liu et al. 2015). The
307 mineralized Jinchuan intrusion were derived from an enriched SCLM source (Li et al. 2005; Li and Ripley
308 2011; Zhang et al. 2013), potentially caused by subduction-related processes (e.g., Song et al. 2018). Slab
309 subduction and dehydration can transport a significant amount of metals from subducted slabs to overlying
310 mantle wedge (e.g., Canil and Fellows 2017).

311 Slab-derived fluids typically have high oxygen fugacity above the sulfide-sulfur oxide buffer (Sun et al.
312 2007). As ^{65}Cu is preferentially leached into fluids when redox reactions happened (e.g., Mathur et al. 2005),
313 dehydration of oceanic crust is expected to enrich ^{65}Cu in the fluids (Huang et al. 2016b). Copper in mantle
314 rocks is mainly controlled by sulfide phases, which are sensitive to metasomatism by melt/fluid–rock
315 interaction (e.g., Lee et al. 2012). Consequently, Cu transportation from oxidized subducted slabs to the
316 SCLM could potentially enrich the mantle sources in heavy Cu isotopes (e.g., Liu et al. 2015; Wang et al.
317 2019). Indeed, pre-enrichment of metals in the mantle source is considered as a favorable process in the
318 generation of a variety of ore deposit types (e.g., Wilkinson 2013).

319 On the other hand, the addition of oxidizing fluids from subducted slabs to the mantle would cause
320 oxidative breakdown of sulfides (e.g., Liu et al. 2015; Huang et al. 2016a, b). In this process, heavier Cu
321 isotopes are preferentially enriched in the released fluids. Precipitation of secondary Cu-bearing sulfide
322 minerals from the ^{65}Cu-rich fluids may shift the peridotites to heavy Cu isotopic compositions (Liu et al.
323 2015). By contrast, metasomatized peridotites that experienced oxidative breakdown of sulfides would be

This is the peer-reviewed, final accepted version for American Mineralogist, published by the Mineralogical Society of America.
The published version is subject to change. Cite as Authors (Year) Title. American Mineralogist, in press.
DOI: https://doi.org/10.2138/am-2021-7911. http://www.minsocam.org/

enriched in lighter Cu isotopes than the primary non-metasomatized rocks. The ^{65}Cu-rich fluids derived from both subducted slabs and subsequent sulfide dissolution in the mantle result in the enrichment of heavy Cu isotopes. The relative contribution of Cu isotope fractionation caused by a subduction event and dissolution of pre-existing Cu-bearing sulfides in the mantle is difficult to estimate. However, our study clearly demonstrates that Cu enrichment in the mantle sources has been involved during the formation of the Jinchuan deposit. An anomalously hot plume rising from the deep mantle may have triggered partial melting of the long-term enriched SCLM in the Jinchuan area (e.g., Li et al. 2005; Li and Ripley 2011; Zhang et al. 2013). Numerical modeling indicates that the SCLM has experienced 17–20% partial melting, during which sulfides were exhausted (e.g., Li and Ripley 2011). Consequently, the SCLM-derived primary magma was fertile in chalcophile elements.

The evolution of Cu isotopes during the formation of the Jinchuan Ni–Cu deposits

The influx of metal-bearing oxidized fluids into the mantle source can cause the enrichment of heavy Cu isotopes in the metasomatized mantle (δ^{65}Cu = 0.54 ± 0.22‰; Stage I, Fig. 8a). The metasomatized mantle-derived magmas inherited heavy Cu isotopic compositions of their sources (δ^{65}Cu = 0.54 ± 0.22‰; Stage I, Fig. 8a). Numerical modeling indicates that the primary magmas of the Jinchuan deposit experienced ~0.008% sulfide liquids removal during its ascent from the mantle to the magma chamber (e.g., Song et al. 2009). Calculations using the Rayleigh equation (Equation 4, $\alpha^{65}Cu_{\text{sulfide melt-magma}}$ = 0.9999, e.g., Savage et al. 2015; Xia et al. 2019) demonstrate that ~0.008% sulfide liquids removal caused limited Cu isotope fractionation (<0.00008‰ for δ^{65}Cu, Stage I, Fig. 8a). Minor olivine crystallization also caused negligible Cu isotope fractionation because of the low partition coefficient between olivine and silicate magma ($D_{olivine/magma}$ = 0.05, Lee et al. 2012).

In the dynamic magma conduit, sulfide melts interacted with a very large volume of metal-bearing magmas (Fig. 6, Equation 2 with R factors from ~500 to ~2700), scavenging of metals from these multiple magma pulses (Duan et al., 2016). Sulfide-magma differentiation would enrich the sulfide melt in lighter Cu isotopes (δ^{65}Cu = 0.44 ± 0.22‰) than the silicate magma (δ^{65}Cu = 0.54 ± 0.22‰; Stage II, Fig. 8b). Settling of sulfide droplets and post-cumulus percolation (e.g., Mao et al. 2018) would cause the sulfide

accumulation in the lower parts of the magma chamber. These accumulated sulfide melts further fractionated into Fe-rich sulfide cumulates (low Pd/Ir and Cu/Ni ratios, Fig. 4b–f) and residual Cu-rich sulfide liquid (high Pd/Ir and Cu/Ni ratios, Fig. 4b–f), contributing to increased δ^{65}Cu values (e.g., Zhao et al. 2017, 2019) from −0.91‰ to +1.29‰ (Stage III, Fig. 8c). The concentrated sulfide melts were fragmented and assimilated by new magma pluses, followed by the second stage of scavenging of metals, sulfide segregation, internal sulfide fractionation, and sulfide percolation, which generated light and variable Cu isotopic compositions (Stage IV, Fig. 8d).

IMPLICATIONS

Geochemical data from large igneous provinces (LIPs) show that "fertile" mantle sources are favorable to formation of magmatic Ni–Cu–(PGE) deposits, whereas LIPs without interactions with ancient SCLM roots are rarely mineralized (Zhang et al. 2008). Most world-class magmatic Ni–Cu–(PGE) deposits occur along craton margins (Begg et al., 2010; Griffin et al. 2013), which implies that interactions between a mantle plume and metasomatized mantle overlying a continental rift provides favorable conditions for giant Ni–Cu–(PGE) mineralization (e.g., Barnes and Lightfoot 2005). The parental magmas of the Jinchuan intrusion are estimated to have an average δ^{65}Cu value of 0.54 ± 0.22‰ (2SD), which is higher than the mantle value of ~0.06‰. Copper transportation from oxidized subducted slabs to mantle peridotites or dissolution of pre-existing Cu-bearing sulfides in the mantle caused oxidative breakdown and reprecipitation of sulfides and shifted the hybridized mantle toward heavier Cu isotopic compositions. Our study indicates that metal enrichment in the metasomatized mantle sources eventually generated primary magmas fertile in chalcophile elements in the Jinchuan magmatic Ni−Cu deposit. It is worth noting that the maximum δ^{65}Cu values of disseminated sulfides from world-class magmatic Ni−Cu deposits (1‰ to 1.84‰) are higher than those of disseminated sulfides from large to small size deposits (−0.17‰ to 0.15‰, Fig. 3). Given that sulfide melts preferentially incorporate lighter Cu isotopes relative to silicate magmas (e.g., Savage et al. 2015; Xia et al. 2019; Liu et al., 2021), the elevated δ^{65}Cu values in magmatic Ni−Cu deposits may be inherited from their mantle sources, but this needs to be clarified by future studies. Metal enrichment in mantle source could be a key step in the generation of giant magmatic Ni–Cu deposits worldwide, especially

This is the peer-reviewed, final accepted version for American Mineralogist, published by the Mineralogical Society of America.
The published version is subject to change. Cite as Authors (Year) Title. American Mineralogist, in press.
DOI: https://doi.org/10.2138/am-2021-7911. http://www.minsocam.org/

for small mafic-ultramafic intrusions.

In porphyry Cu systems, chalcopyrites from hypogene ores have δ^{65}Cu values that average 0‰ (Mathur et al. 2009). Experimental studies indicate that exsolved fluids have higher δ^{65}Cu than those of the magmas (Guo et al., 2020), while the vapors removed via boiling are enriched in lighter Cu isotopes relative to the deeper, brine-rich source of the ore-forming fluids (Rempel et al. 2012). Thus, careful considerations of these processes in porphyry Cu systems should be constrained before the Cu isotopic compositions of hypogene sulfides can be used to track magma sources. By taking all important processes into account, the elevated δ^{65}Cu values of porphyries and mafic magmatic enclaves (MMEs) from giant porphyry Cu deposits in southern Tibet suggest initial Cu enrichment in their magma sources (e.g., Zheng et al. 2019).

Copper isotopes, in combination with PGE geochemistry, can be utilized to estimate the Cu isotopic compositions of parental/primary magmas and mantle sources for magmatic Ni–Cu deposits. Since sulfides incorporate lighter Cu isotopes than the coexisting magmas (e.g., Savage et al. 2015; Huang et al. 2016a; Zhao et al. 2017, 2019; Xia et al. 2019), the significant enrichment of heavy Cu isotopes in disseminated sulfides in magmatic Ni–Cu deposits was potentially inherited from their metasomatized and metal-rich mantle sources. Thus, Cu isotopes can be considered as a reliable tracer for tracking metal enrichment in mantle source and shed new light on further mineral exploration, even though the influence of crustal contamination, diffusion and mineralization process must be taken into account.

ACKNOWLEDGEMENTS

We thank Yushan Wang, Qixing Ai, Yalin Gao, Qijin Ju, Kaiwu Zha and Junchao Wang of the Jinchuan Group Co. Ltd for their help in field work. We are grateful for Prof. David T.A. Symons of University of Windsor, who provided final language editing. Critical comments from Prof. Ryan Mathur and Dr. Xin Ding, and editorial inputs from Prof. William H. Peck are greatly appreciated. This study was jointly funded by the National Key R&D Program of China (2017YFC0601202), National Natural Science Foundation of China (41803013 and 41473017), State Key Laboratory for Mineral Deposits Research (2021-LAMD-K10) and Fundamental Research Funds for the Central Universities (QZ05201905 and 2652019050).

REFERENCES CITED

Asif, M., and Parry, S.J. (1991) Study of the digestion of chromite during nickel sulphide fire assay for the platinum group elements and gold. Analyst, 116, 1071–1073.

Balaram, V., Anjaiah, K.V., and Reddy, M.R.P. (1995) Comparative study on the trace and rare earth element analysis of an Indian polymetallic nodule reference sample by inductively coupled plasma atomic emission spectrometry and inductively coupled plasma mass spectrometry. Analyst, 120, 1401–1406.

Barnes, S.J., and Lightfoot, P.C. (2005) Formation of magmatic nickel sulfide ore deposits and processes affecting their copper and platinum group element contents. Economic Geology 100th Anniversary Volume, 179–213.

Barnes, S.J., and Maier, W.D. (1999) The fractionation of Ni, Cu and the noble metals in silicate and sulfide liquids. Short Course Notes, vol. 13. Geological Association of Canada, pp. 69–106.

Begg, G.C., Hronsky, J.A.M., Arndt, N.T., Griffin, W.L., O'Reilly, S.Y., and Hayward, N. (2010) Lithospheric, cratonic, and geodynamic setting of Ni–Cu–PGE sulfide deposits. Economic Geology, 105, 1057–1070.

Brzozowski, M.J., Good, D.J., Wu, C.Z., and Li W.Q. (2020). Cu isotope systematics of conduit-type Cu–PGE mineralization in the Eastern Gabbro, Coldwell Complex, Canada. Mineralium Deposita, https://doi.org/10.1007/s00126-020-00992-8

Canil, D., and Fellows, S.A. (2017). Sulphide–sulphate stability and melting in subducted sediment and its role in arc mantle redox and chalcophile cycling in space and time. Earth and Planetary Science Letters, 470, 73–86.

Campbell, I.H., and Naldrett, A.J. (1979) The influence of silicate: sulfide ratios on the geochemistry of magmatic sulfides. Economic Geology, 74, 1503–1506.

Chen, L.M., Song, X.Y., Reid, R.K., Tian, Y.L., Wang, Y.S., Deng, Y.F., and Xiao, J.F. (2013) Segregation and fractionation of magmatic Ni–Cu–PGE sulfides in the Western Jinchuan Intrusion, Northwestern China: insights from platinum group element geochemistry. Economic Geology, 108, 1793–1811.

Ding, X., Ripley, E. M., Underwood, B. S., Meng, Z., and Huang, F. (2021). Behavior of Mg and CO isotopes during mafic magma-carbonate interaction at the Jinchuan Ni–Cu deposit, North China Craton.

Chemical Geology, 562, 120044.

Duan, J., Li, C., Qian, Z., Jiao, J., Ripley, E. M., and Feng, Y.. (2016). Multiple S isotopes, zircon Hf isotopes, whole-rock Sr-Nd isotopes, and spatial variations of PGE tenors in the Jinchuan Ni–Cu–PGE deposit, NW China. Mineralium Deposita, 51(4), 557−574.

Fiorentini, M.L., and Beresford, S.W. (2008). Role of volatiles and metasomatized subcontinental lithospheric mantle in the genesis of magmatic Ni–Cu–PGE mineralization: insights from in situ H, Li, B analyses of hydromagmatic phases from the Valmaggia ultramafic pipe, Ivrea-Verbano Zone (NW Italy). Terra Nova, 20(5), 333−340.

Griffin, W. L., Begg, G.C., and O'reilly, S.Y. (2013). Continental-root control on the genesis of magmatic ore deposits. Nature Geoscience, 6(11), 905−910.

Guo, H., Xia, Y., Bai, R., Zhang, X., and Huang, F. (2020). Experiments on Cu-isotope fractionation between chlorine-bearing fluid and silicate magma: implications for fluid exsolution and porphyry Cu deposits. National Science Review, 7(8), 1319–1330.

Huang, J., Liu, S.-A., Wörner, G., Yu, H., and Xiao, Y. (2016a) Copper isotope behavior during extreme magma differentiation and degassing: a case study on Laacher See phonolite tephra (East Eifel, Germany). Contributions to Mineralogy and Petrology, 171, 76.

Huang, J., Liu, S.-A., Gao, Y., Xiao, Y., and Chen, S. (2016b). Copper and zinc isotope systematics of altered oceanic crust at IODP Site 1256 in the eastern equatorial Pacific. Journal of Geophysical Research Solid Earth, 121, 7086–7100.

Huang, J., Huang, F., Wang, Z., Zhang, X., and Yu, H. (2017). Copper isotope fractionation during partial melting and melt percolation in the upper mantle: Evidence from massif peridotites in Ivrea-Verbano Zone, Italian Alps. Geochimica et Cosmochimica Acta, 211, 48–63.

Jugo, P.J. (2009). Sulfur content at sulfide saturation in oxidized magmas. Geology 37(5), 415–418.

Lee, C.-T.A., Luffi, P., Chin, E.J., Bouchet, R., Dasgupta, R., Morton, D.M., Le Roux, V., Yin, Q.-Z., and Jin, D. (2012) Copper Systematics in Arc Magmas and Implications for Crust-Mantle Differentiation. Science, 336, 64–68.

Li, C., and Ripley, E.M. (2011). The giant Jinchuan Ni-Cu-(PGE) deposit; tectonic setting, magma evolution,

ore genesis, and exploration implications. Reviews in Economic Geology, 17, 163–180.

Li, W.Q., Jackson, S.E., Pearson, N.J., Alard, O., and Chappell, B.W. (2009). The Cu isotopic signature of granites from the Lachlan fold belt, SE Australia. Chemical Geology, 258, 38–49.

Li, X. H., Su, L., Chung, S. L., Li, Z. X., Liu, Y., Song, B., and Liu, D. Y. (2005). Formation of the Jinchuan ultramafic intrusion and the world's third largest Ni-Cu sulfide deposit: Associated with the ~825 Ma south China mantle plume?. Geochemistry, Geophysics, Geosystems, 6(11).

Liu, S., Li, Y., Liu, J., Yang, Z., Liu, J., and Shi, Y. (2021). Equilibrium Cu isotope fractionation in copper minerals: a first-principles study. Chemical Geology, 120060.

Liu, S.-A., Li, D.D., Li, S.G., Teng, F.Z., Ke, S., He, Y.S., and Lu, Y.H. (2014a) High-precision copper and iron isotope analysis of igneous rock standards by MC-ICP-MS. Journal of Analytical Atomic Spectrometry, 29, 122–133.

Liu, S. A., Liu, P. P., Lv, Y., Wang, Z. Z., and Dai, J. G. (2019). Cu and Zn isotope fractionation during oceanic alteration: implications for Oceanic Cu and Zn cycles. Geochimica et Cosmochimica Acta, 257, 191–205.

Liu, S.-A., Huang, J., Liu, J.G., G. Wörner., Yang, W., Tang, Y.J., Chen, Y., Tang, L.-M., Zheng, J.P., and Li, S.-G. (2015) Copper isotopic composition of the silicate Earth. Earth and Planetary Science Letters, 427, 95–103.

Liu, S. A., Teng, F. Z., Li, S., Wei, G. J., Ma, J. L., and Li, D. (2014b). Copper and iron isotope fractionation during weathering and pedogenesis: insights from saprolite profiles. Geochimica et Cosmochimica Acta, 146, 59–75.

Malitch, K.N., Latypov, R. M., Badanina, I.Y., and Sluzhenikin, S.F. (2014) Insights into ore genesis of Ni–Cu–PGE sulfide deposits of the Noril' sk Province (Russia): Evidence from copper and sulfur isotopes. Lithos, 204, 172–187.

Maier, W.D., and Barnes, S.-J. (2004) Pt/Pd and Pd/Ir ratios in mantle-derived magmas: A possible role for mantle metasomatism. South African Journal of Geology, 107, 333−340.

Mathur, R., Ruiz, J., Titley, S., Liermann, L., Buss, H., and Brantley, S. (2005) Cu isotopic fractionation in the supergene environment with and without bacteria. Geochimica et Cosmochimica Acta, 69(22),

5233–5246.

Mathur, R., Titley, S., Barra, F., Brantley, S., Wilson, M., Phillips, A., Munizaga, F., Maksaev, V., Vervoort, J., and Hart, G. (2009). Exploration potential of Cu isotope fractionation in porphyry copper deposits. Journal of Geochemical exploration, 102(1), 1–6.

Mao, Y.J., Barnes, S.J., Duan, J., Qin, K.Z., Godel, B.M., and Jiao, J. (2018). Morphology and particle size distribution of olivines and sulphides in the Jinchuan Ni–Cu sulphide deposit: Evidence for sulphide percolation in a crystal mush. Journal of Petrology, 59(9), 1701–1730.

McDonough, W.F., and Sun, S.S. (1995) The composition of the earth. Chemical Geology 120, 223–253.

Moynier, F., Vance, D., Fujii, T., and Savage, P. (2017). The isotope geochemistry of zinc and copper. Reviews in Mineralogy and Geochemistry, 82(1), 543–600.

Mungall, J.E., and Brenan, J.M. (2014) Partitioning of platinum-group elements and Au between sulfide liquid and basalt and the origins of mantle-crust fractionation of the chalcophile elements. Geochimica et Cosmochimica Acta, 125, 265–289.

Naldrett, A.J. (2010) From the mantle to the bank: the life of a Ni-Cu-(PGE) sulfide deposit. South African Journal of Geology, 113, 1–32.

Neumann, H., Mead J. and Vitaliano C.J. (1954) Trace element variation during fractional crystallization as calculated from the distribution law. Geochimica et Cosmochimica Acta, 6, 90−99.

Rehkaemper, M., Halliday, A.N., Fitton, J.G., Lee, D.C., Wieneke, M., and Arndt, N.T. (1999). Ir, Ru, Pt, and Pd in basalts and komatiites: new constraints for the geochemical behavior of the platinum-group elements in the mantle. Geochimica et Cosmochimica Acta, 63(22), 3915–3934.

Rempel, K. U., Liebscher, A., Meixner, A., Romer, R. L., and Heinrich, W. (2012). An experimental study of the elemental and isotopic fractionation of copper between aqueous vapour and liquid to 450 °C and 400 bar in the CuCl–NaCl–H_2O and CuCl–NaHS–NaCl–H_2O systems. Geochimica et Cosmochimica Acta, 94, 199–216.

Richardson, S.H., and Shirey, S.B. (2008). Continental mantle signature of Bushveld magmas and coeval diamonds. Nature, 453, doi:10.1038/nature07073.

Richter, F. M., Davis, A. M., DePaolo, D. J., and Watson, E. B. (2003). Isotope fractionation by chemical

513 diffusion between molten basalt and rhyolite. Geochimica et Cosmochimica Acta, 67(20), 3905-3923.

514 Ripley, E.M., Brophy, J.G., and Li, C. (2002) Copper solubility in a basaltic melt and sulfide liquid/silicate
515 melt partition coefficients of Cu and Fe. Geochimica et Cosmochimica Acta, 66(15), 2791–2800.

516 Ripley, E. M., Sarkar, A., and Li, C. (2005). Mineralogic and stable isotope studies of hydrothermal
517 alteration at the Jinchuan Ni-Cu deposit, China. Economic Geology, 100(7), 1349–1361.

518 Ripley, E.M., Dong, S.F., Li, C.S., and Wasylenki, L.E. (2015) Cu isotope variations between conduit and
519 sheet-style Ni-Cu-PGE sulfide mineralization in the Midcontinent Rift System, North America.
520 Chemical Geology, 414, 59–68. Rudnick, R. L., and Gao, S. (2003). Composition of the continental
521 crust. Treatise on geochemistry, 3, 659.

522 Savage, P.S., Moynier, F., Chen, H., Shofner, G., Siebert, J., Badro, J., and Puchtel, I.S. (2015) Copper
523 isotope evidence for large-scale sulphide fractionation during Earth's differentiation. Geochemical
524 Perspectives Letters, 1, 52–64.

525 Sun, X., Tang, Q., Sun, W., Xu, L., Zhai, W., Liang, J., Liang, Y., Shen, K., Zhang, Z., and Zhou B. (2007)
526 Monazite, iron oxide and barite exsolutions in apatite aggregates from CCSD drillhole eclogites and
527 their geological implications. Geochimica et Cosmochimica Acta, 71, 2896–2905.

528 Song, X.Y., Keays, R.R., Zhou, M.F., Qi, L., Ihlenfeld, C., and Xiao, J.F. (2009) Siderophile and chalcophile
529 elemental constraints on the origin of the Jinchuan Ni-Cu-(PGE) sulfide deposit, NW China.
530 Geochimica et Cosmochimica Acta, 73, 404−424.

531 Song, X.Y., Hu, R.Z., and Chen, L.M. (2018) Characteristics and inspirations of the Ni–Cu sulfide deposits
532 in China. Journal of Nanjing University. Natural Sciences, 54(2), 221−235 (in Chinese with English
533 abstract).

534 Sossi, P. A., Halverson, G. P., Nebel, O., and Eggins, S. M. (2015). Combined separation of Cu, Fe and Zn
535 from rock matrices and improved analytical protocols for stable isotope determination. Geostandards
536 and Geoanalytical Research, 39(2), 129-149.

537 Tang, D., Qin, K., Su, B., Mao, Y., Evans, N.J., Niu, Y., and Kang, Z. (2020) Sulfur and copper isotopic
538 signatures of chalcopyrite at Kalatongke and Baishiquan: insights into the origin of magmatic Ni-Cu
539 sulfide deposits. Geochimica et Cosmochimica Acta, doi: https://doi.org/10.1016/j.gca.2020.02.015

Tang, Q., Bao, J., Dang, Y., Ke, S., and Zhao, Y. (2018). Mg–Sr–Nd isotopic constraints on the genesis of the giant Jinchuan Ni–Cu–(PGE) sulfide deposit, NW China. Earth and Planetary Science Letters, 502, 221–230.

Tang ZL, Song X-Y, and Su, S. (2009) Ni–Cu deposits related to high Mg basaltic magma, Jinchuan, western China. In: Li C, Ripley EM (eds) New developments in magmatic Ni-Cu and PGE deposits. Geological Publishing House, Beijing, pp 121–140

Wang, Z., Park, J. W., Wang, X., Zou, Z., Kim, J., Zhang, P., and Li, M. (2019). Evolution of copper isotopes in arc systems: Insights from lavas and molten sulfur in Niuatahi volcano, Tonga rear arc. Geochimica et Cosmochimica Acta, 250, 18–33.

Williams, H.M., and Archer, C. (2011) Copper stable isotopes as tracers of metal-sulphide segregation and fractional crystallisation processes on iron meteorite parent bodies. Geochimica et Cosmochimica Acta, 75, 3166–3178.

Wilkinson, J.J. (2013). Triggers for the formation of porphyry ore deposits in magmatic arcs. Nature Geoscience, 6(11), 917-925.

Xia, Y., Kiseeva, E. S., Wade, J., and Huang, F. (2019) The effect of core segregation on the Cu and Zn isotope composition of the silicate Moon. Geochemical Perspectives Letters, 12, 12–17.

Zhao, Y., Xue, C.J, Liu, S.-A., Symons, D. T., Zhao, X.B, Yang, Y.Q., and Ke, J.J. (2017) Copper isotope fractionation during sulfide-magma differentiation in the Tulaergen magmatic Ni–Cu deposit, NW China. Lithos, 286–287C, 206–215.

Zhao, Y., Xue, C. J., Liu, S. A., Mathur, R., Zhao, X. B., Yang, Y. Q., Dai, J.F., Man, R.H., and Liu, X.M (2019) Redox reactions control Cu and Fe isotope fractionation in a magmatic Ni–Cu mineralization system. Geochimica et Cosmochimica Acta, 249, 42–58.

Zhang, M., Tang, Q., Hu, P., Ye, X., and Cong, Y. (2013). Noble gas isotopic constraints on the origin and evolution of the Jinchuan Ni–Cu–(PGE) sulfide ore-bearing ultramafic intrusion, Western China. Chemical Geology, 339, 301−312.

Zhang, M., O'Reilly, S.Y., Wang, K., Hronsky, J., and Griffn, W.L. (2008). Flood basalts and metallogeny: The lithospheric mantle connection. Earth Science Reviews, 86, 145−174.

567 Zheng, Y. C., Liu, S. A., Wu, C. D., Griffin, W. L., Li, Z. Q., Xu, B., and O'Reilly, S. Y. (2019). Cu isotopes
568 reveal initial Cu enrichment in sources of giant porphyry deposits in a collisional setting. Geology, 47,
569 135−138.

570

This is the peer-reviewed, final accepted version for American Mineralogist, published by the Mineralogical Society of America.
The published version is subject to change. Cite as Authors (Year) Title. American Mineralogist, in press.
DOI: https://doi.org/10.2138/am-2021-7911. http://www.minsocam.org/

FIGURE CAPTIONS

FIGURE 1 (a) The major tectonic units of China with the Jinchuan Ni–Cu deposit indicated. (b) Geological maps of the Jinchuan intrusion and (c) a projected section, modified from Li and Ripley (2011), Duan et al. (2016) and Mao et al. (2018).

FIGURE 2 (a) Disseminated sulfide mineralization including chalcopyrite, pyrrhotite and pentlandite. (b) Net-textured sulfides with a large number of chalcopyrite, but minor pyrrhotite and pentlandite. (c) Massive sulfides with Cu-rich and Fe-rich zonation. (d) Coexistence of chalcopyrite, pyrrhotite and pentlandite in massive sulfides. Abbreviations: Ccp = chalcopyrite, Po = pyrrhotite, Pn = pentlandite.

FIGURE 3 The δ^{65}Cu ranges of bulk silicate Earth (BSE, vertical black dotted line and green bar), metasomatized peridotite, non-metasomatized peridotite, magmatic Ni–Cu deposits including Midcontinent Rift System (Ripley et al. 2015), Noril'sk Province (Malitch et al. 2014), Eastern Gabbro (Brzozowski et al. 2020), Tulaergen (Zhao et al. 2017, 2019), Kalatongke (Tang et al. 2020), Baishiquan (Tang et al. 2020) and Jinchuan (this study). The estimated initial sulfide melts and parental magma for the Jinchuan deposit are also indicated.

FIGURE 4 (a) The projected long section with sample locations indicated. (b) The Pd/Ir_{100} and (c) Cu/Ni_{100} ratios as a function of sample locations. (d–f) Primitive mantle-normalized Ni_{100}, PGE_{100} and Cu_{100} patterns of sulfide ores in the Jinchuan intrusion. These elements are in 100% sulfide. The values of primitive mantle are cited from Barnes and Maier (1999) and McDonough and Sun (1995).

FIGURE 5 (a) The projected long section with sample locations indicated. (b) Cu isotopic composition as a function of sample locations (error bars are smaller than symbols). (c) Cu isotopic compositions of four repeated chalcopyrite samples.

This is the peer-reviewed, final accepted version for American Mineralogist, published by the Mineralogical Society of America.
The published version is subject to change. Cite as Authors (Year) Title. American Mineralogist, in press.
DOI: https://doi.org/10.2138/am-2021-7911. http://www.minsocam.org/

598 **FIGURE** 6 Modeling of Pd vs. Ir contents in 100% sulfide at variable R-factors (Campbell and Naldrett
599 1979) and sulfide-melt fractionation. The partition coefficients are within experiment ranges (Barnes and
600 Lightfoot 2005). Parental magmas of the Jinchuan Ni–Cu deposit contain 0.49 ppb Pd and 0.14 ppb Ir. For
601 comparison, the parental magma of the Tulaergen deposit (grey line) is provided (0.25 ppb Pd and 0.003 ppb
602 Ir, Zhao et al. 2019).
603
604 **FIGURE** 7 Diagrams illustrating the variation between (a) Cu and S contents, (b) Cu contents and δ^{65}Cu
605 values, (c) Cu/Ni ratio and δ^{65}Cu values, and (d) Pd/Ir ratio and δ^{65}Cu values in the Jinchuan deposit
606 (symbols are larger than error bars). The Cu, Ni and S contents are in 100% sulfide. The parameters for
607 numerical modeling are listed in Table 1. Two groups of isotope fractionation factor were set for comparison,
608 including ($\alpha^{65}Cu_{\text{MSS–sulfide melt}}$= 0.9990 and $\alpha^{65}Cu_{\text{residual sulfide melt–sulfide melt}}$ = 1.0010) and ($\alpha^{65}Cu_{\text{MSS–sulfide melt}}$=
609 0.9998 and $\alpha^{65}Cu_{\text{residual sulfide melt–sulfide melt}}$ = 1.0002), the first of which matched the Jinchuan sulfides better.
610 The Cu and S contents (MORB, Barnes and Lightfoot 2005; Jugo 2009) and Pd/Ir ratio (Rehkaemper et al.
611 1999) of the normal primary magma are marked. Note that normal primary magma refers to the magma
612 derived from partial melting of the depleted/primitive mantle, instead of the primary magma for the Jinchuan
613 deposit. The detailed descriptions for Stage I–IV are given in the text and Fig.8.
614
615 **FIGURE** 8 A model illustrating Cu isotope fractionation in the Jinchuan Ni–Cu deposit, China. Stage I:
616 Partial melting of the SCLM generating primary and parental magma incorporating heavy Cu isotopes;
617 Stage II: Sulfide segregation with enrichment of light Cu isotopes, leaving heavy Cu isotopes in evolved
618 magmas; Stage III: Internal fractionation within segregated sulfide resulted in heavy Cu isotopes preferring
619 residual Cu-rich sulfide melts to Fe-rich sulfide cumulates; Stage IV: Concentrated sulfide melts were
620 fragmented and assimilated by new magma pluses, and the new-formed sulfides would have lighter and
621 more variable Cu isotopic compositions.

This is the peer-reviewed, final accepted version for American Mineralogist, published by the Mineralogical Society of America.
The published version is subject to change. Cite as Authors (Year) Title. American Mineralogist, in press.
DOI: https://doi.org/10.2138/am-2021-7911. http://www.minsocam.org/

622 **TABLE 1.** The fractionation factors and partition coefficients between different phases and Cu isotopic compositions for primary magma, parental magma
623 and initial sulfide melt of the Jinchuan deposit, NW China.

Fractionation factors	Reference	Partition coefficients	Reference	δ^{65}Cu (‰)	Reference
$\alpha^{65}Cu_{\text{residual sulfide melt–sulfide melt}} = 1.0010$	Zhao et al. 2019	$D_{\text{Ir sulfide melt/MSS}} = 1/3.5$, $D_{\text{Pd sulfide melt/MSS}} = 10$, $D_{\text{Cu sulfide melt/MSS}} = 5$, $D_{\text{Ni sulfide melt/MSS}} = 1.25$	Barnes and Lightfoot 2005	Normal primary magma, 0.06 ± 0.20‰	Liu et al. 2015
$\alpha^{65}Cu_{\text{MSS–sulfide melt}} = 0.9990$	Zhao et al. 2019	$D_{\text{Ir MSS/sulfide melt}} = 3.5$, $D_{\text{Pd MSS/sulfide melt}} = 0.1$, $D_{\text{Cu MSS/sulfide melt}} = 0.2$, $D_{\text{Ni MSS/sulfide melt}} = 0.8$	Barnes and Lightfoot 2005	Parental magma, 0.54 ± 0.22‰	This study
$\alpha^{65}Cu_{\text{sulfide melt–magma}} = 0.9999$	Savage et al. 2015; Xia et al. 2019	$D_{\text{Ir sulfide/silicate melt}} = 30000$, $D_{\text{Pd sulfide/silicate melt}} = 20000$, $D_{\text{Cu sulfide/silicate melt}} = 500$, $D_{\text{Ni sulfide/silicate melt}} = 1000$	Barnes and Lightfoot 2005	Initial sulfide melt, 0.44 ± 0.22‰	This study

624

Zhao et al. Figure 1

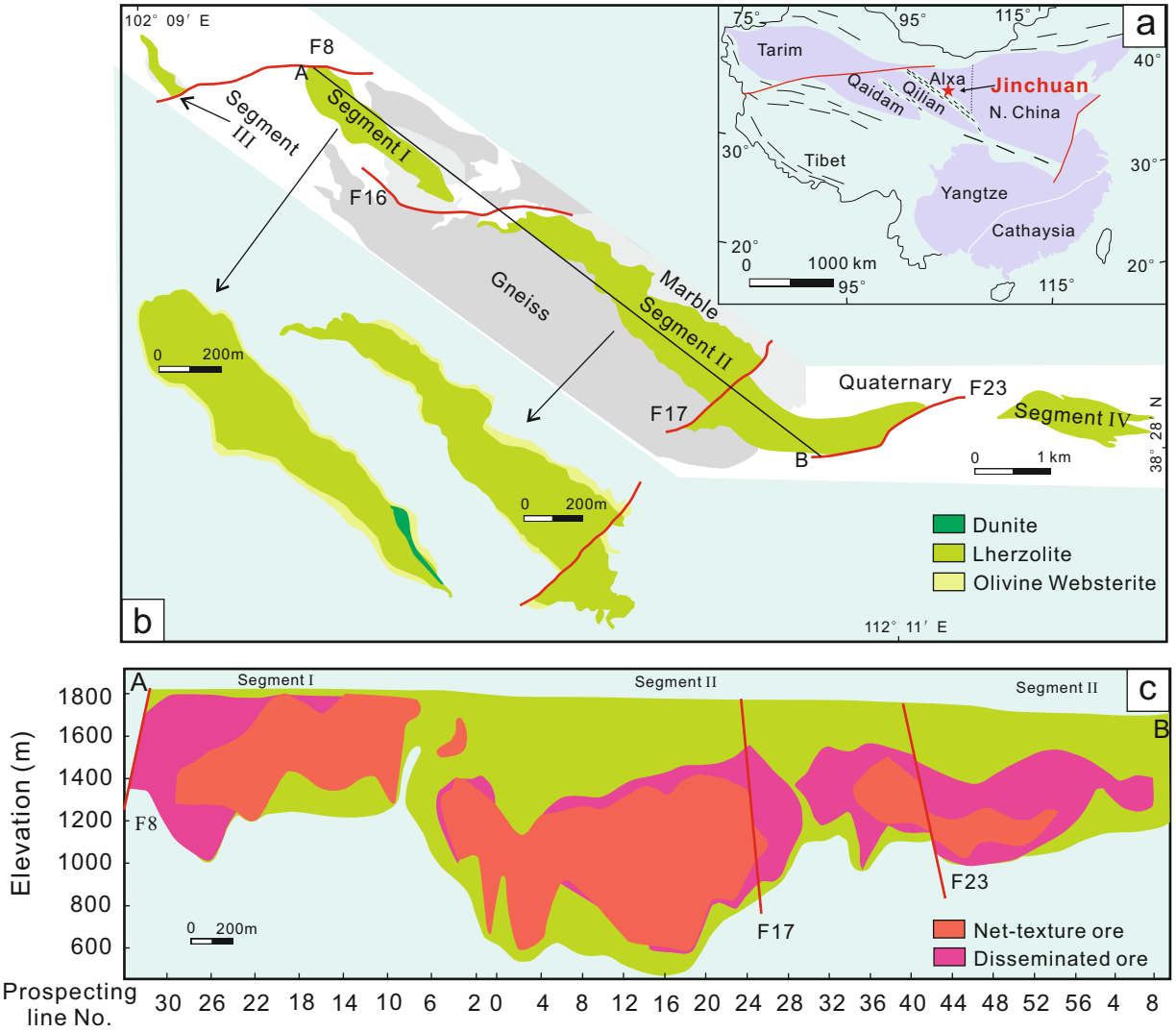

Zhao et al. Figure 2

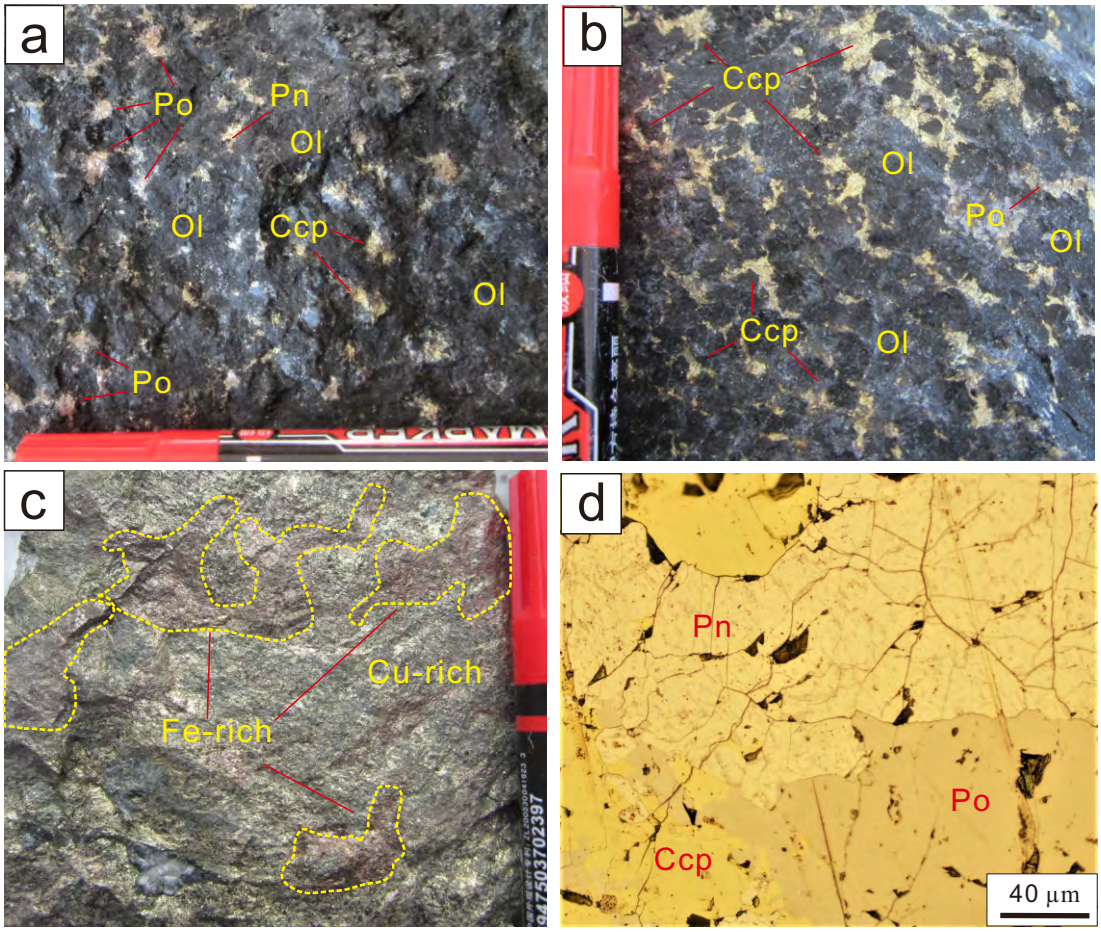

Zhao et al. Figure 3

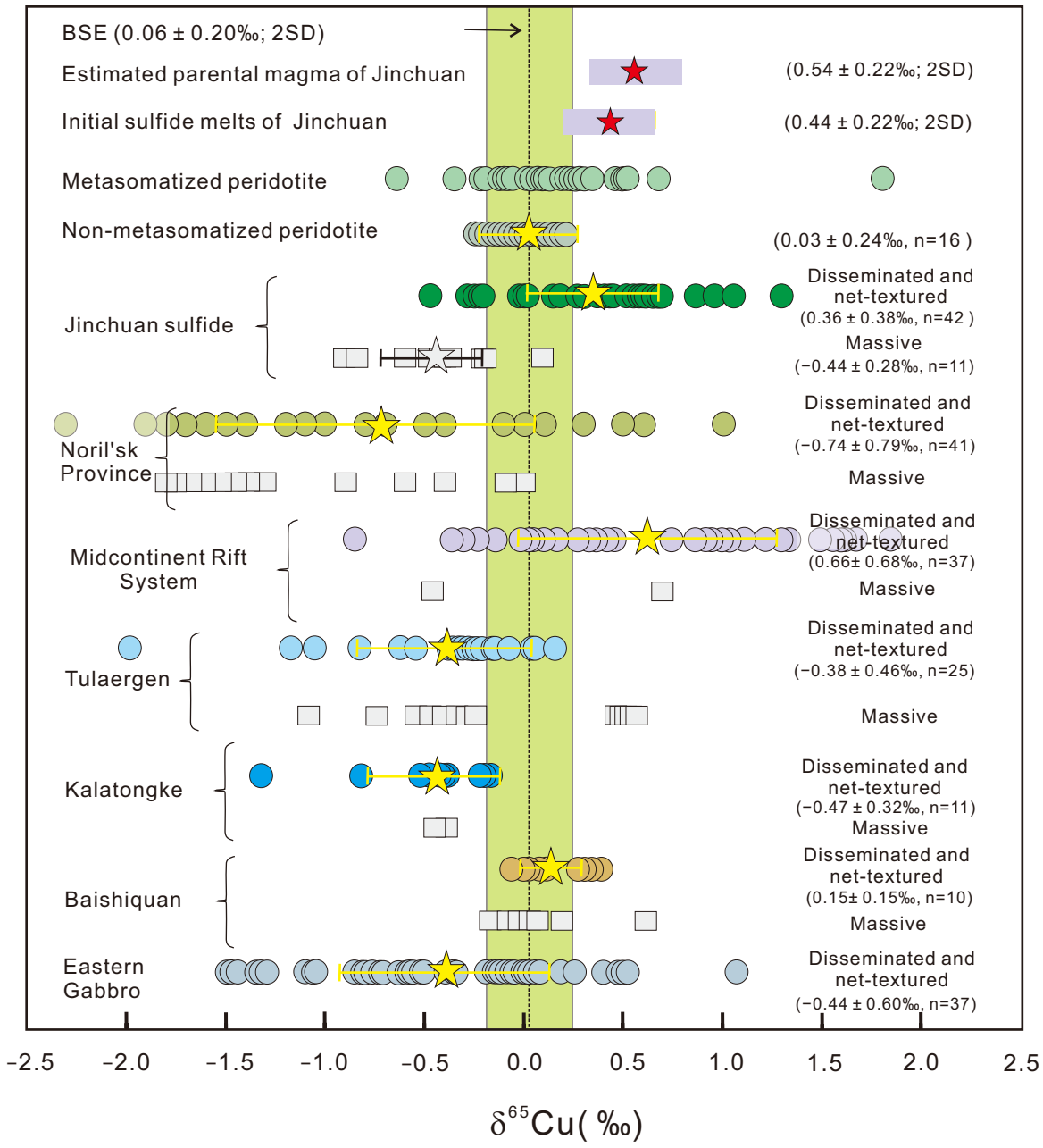

Zhao et al. Figure 4

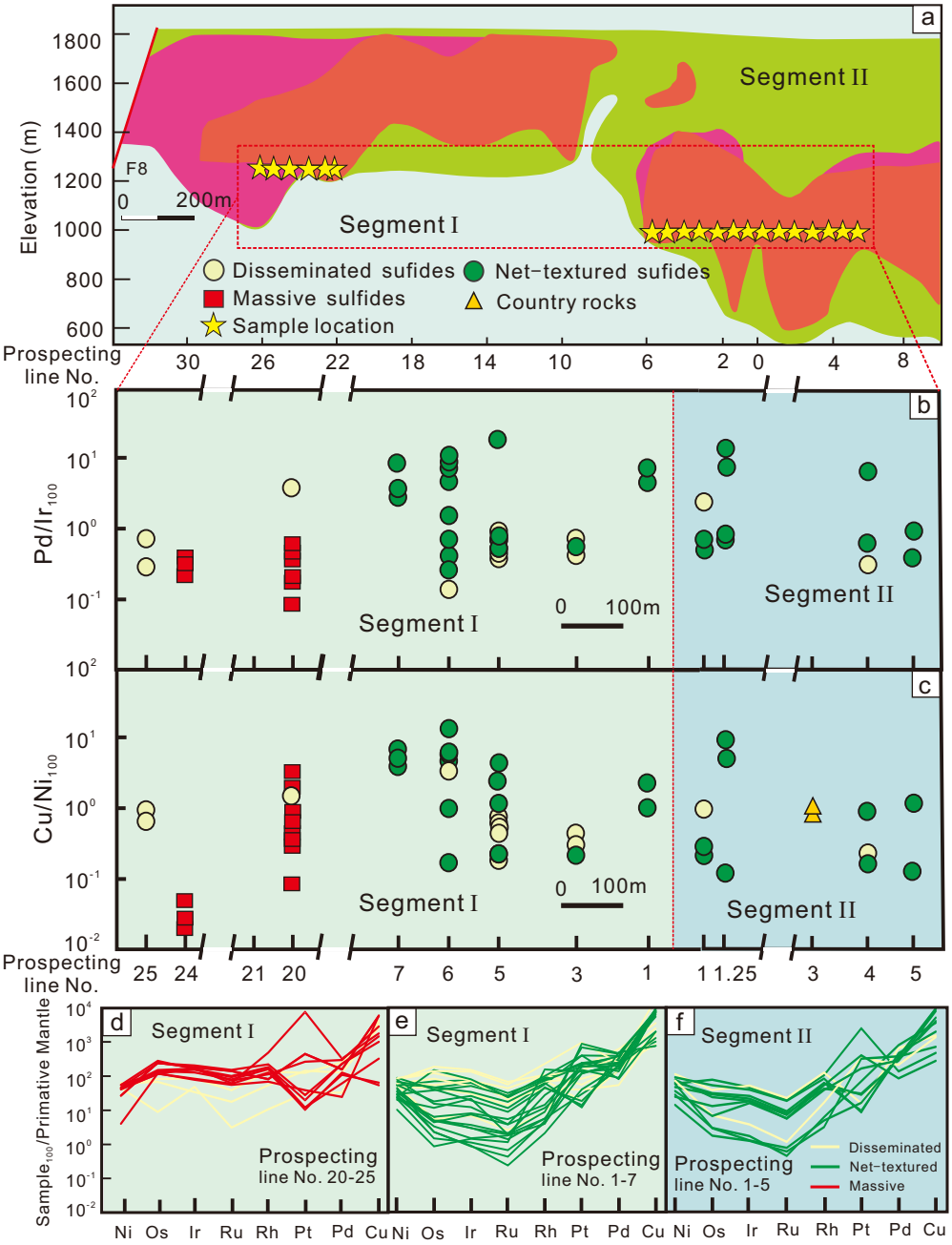

Zhao et al. Figure 5

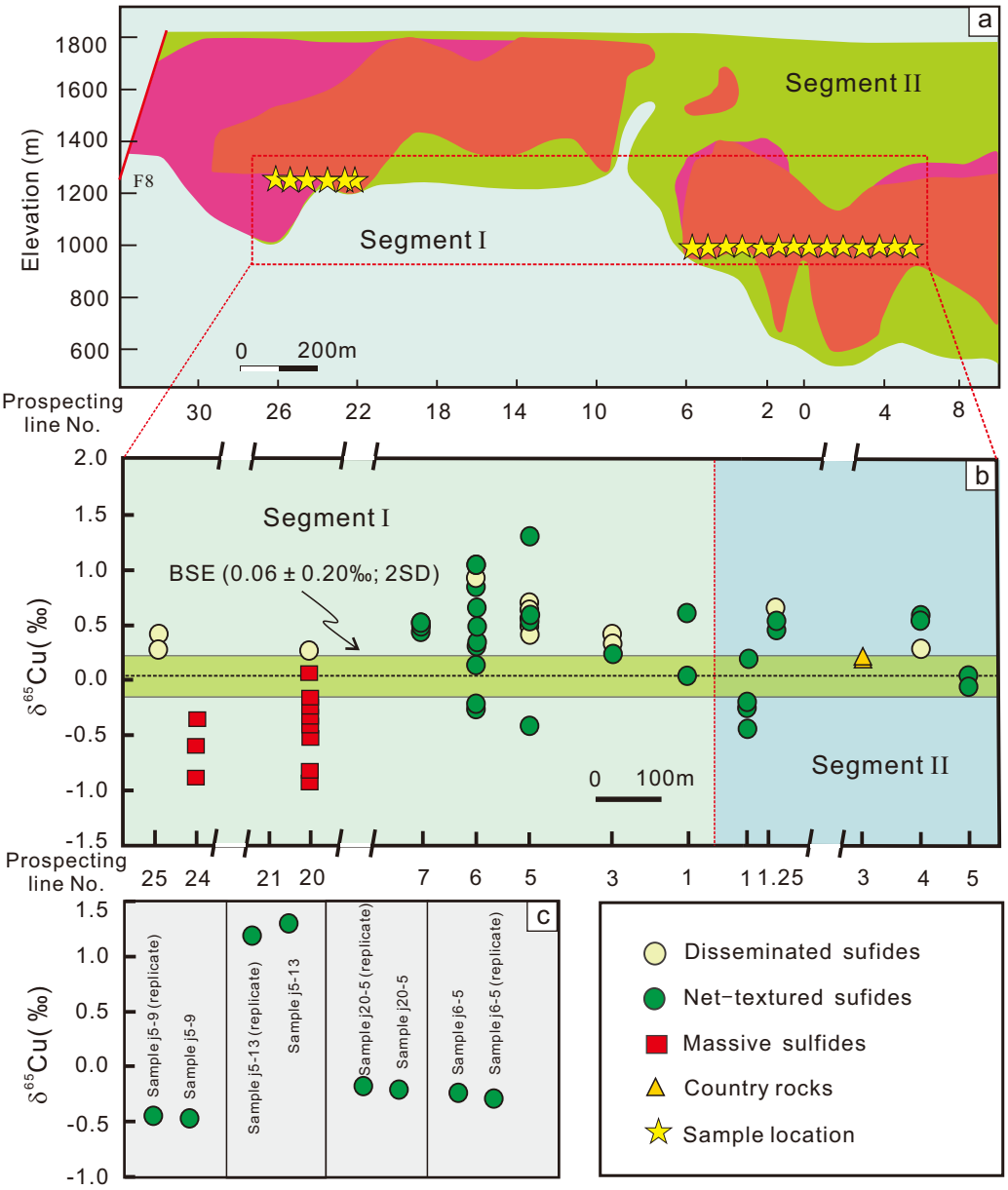

This is the peer-reviewed, final accepted version for American Mineralogist, published by the Mineralogical Society of America.
The published version is subject to change. Cite as Authors (Year) Title. American Mineralogist, in press.
DOI: https://doi.org/10.2138/am-2021-7911. http://www.minsocam.org/

Zhao et al. Figure 6

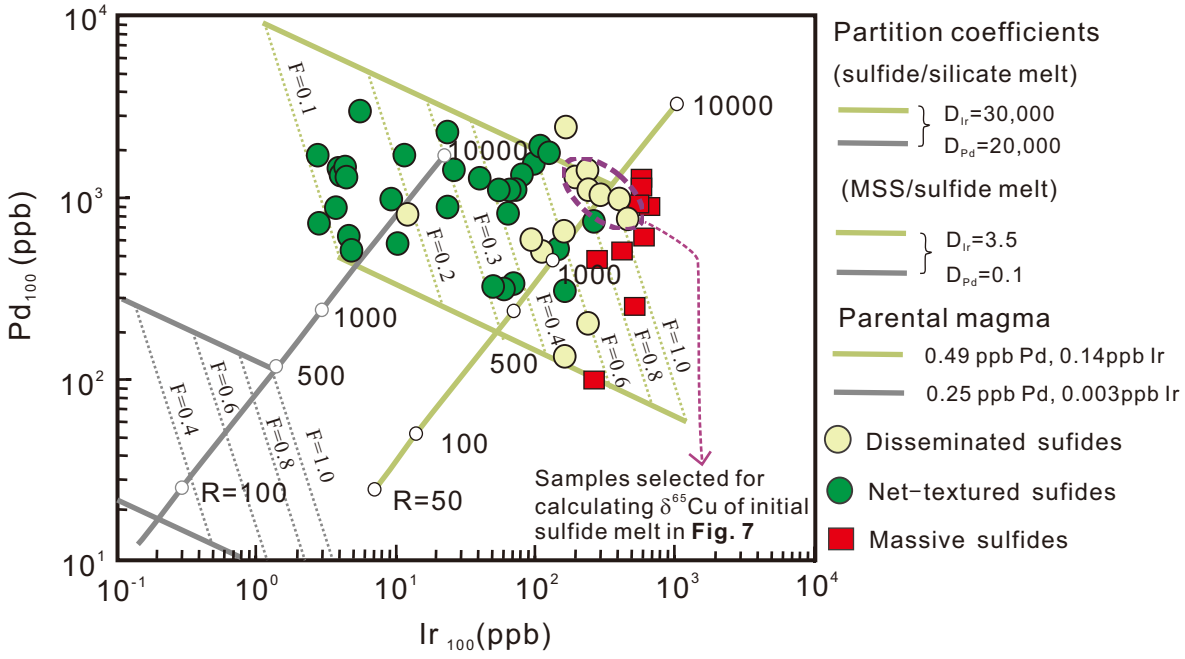

This is the peer-reviewed, final accepted version for American Mineralogist, published by the Mineralogical Society of America.
The published version is subject to change. Cite as Authors (Year) Title. American Mineralogist, in press.
DOI: https://doi.org/10.2138/am-2021-7911. http://www.minsocam.org/

Zhao et al. Figure 7

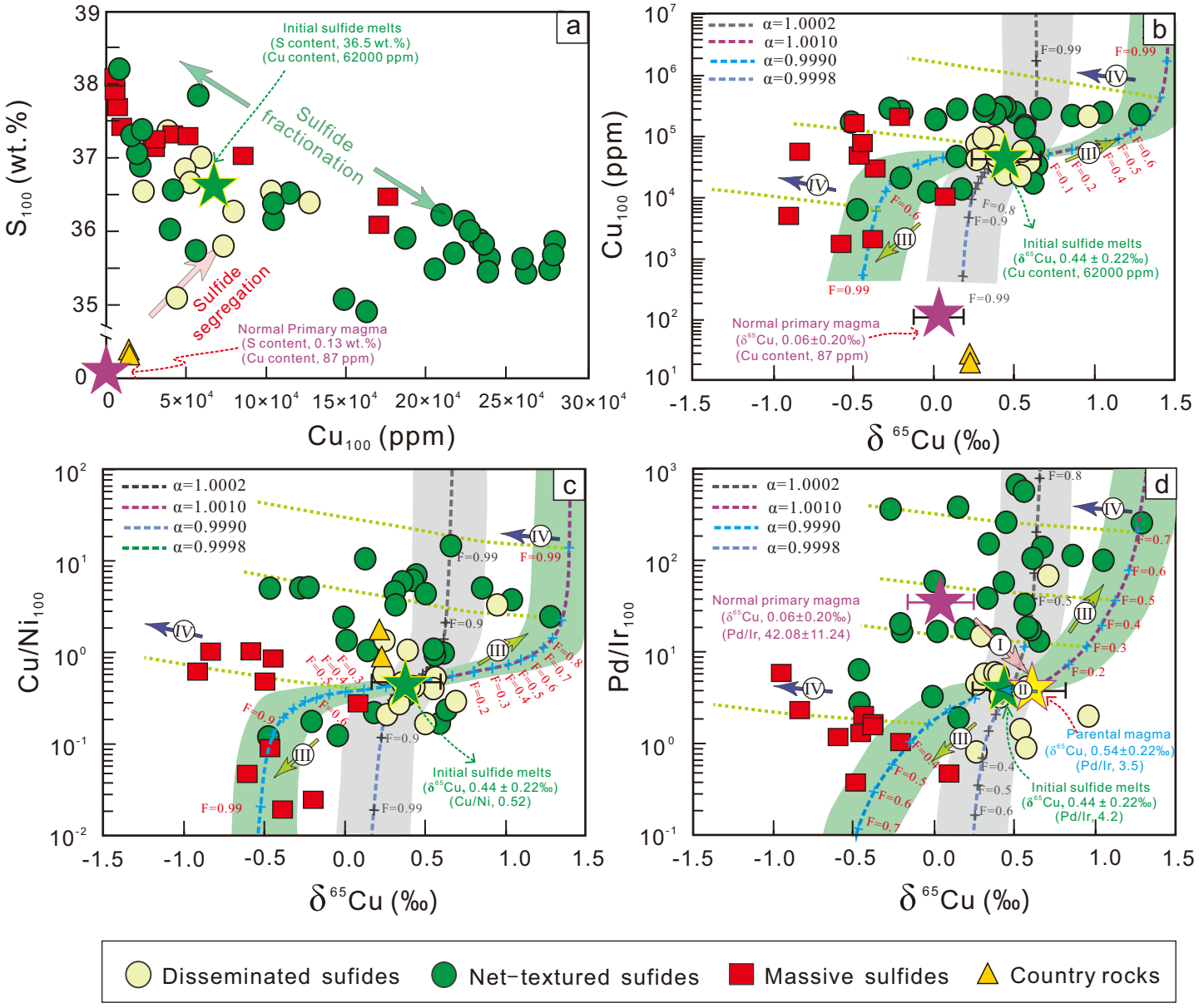

This is the peer-reviewed, final accepted version for American Mineralogist, published by the Mineralogical Society of America.
The published version is subject to change. Cite as Authors (Year) Title. American Mineralogist, in press.
DOI: https://doi.org/10.2138/am-2021-7911. http://www.minsocam.org/

Zhao et al. Figure 8